



Published in final edited form as:

Circ Heart Fail. 2011 January ; 4(1): 89–97. doi:10.1161/CIRCHEARTFAILURE.110.957258.

Delta-Sarcoglycan Gene Therapy Halts Progression of Cardiac Dysfunction, Improves Respiratory Failure and Prolongs Life in Myopathic Hamsters

Masahiko Hoshijima, MD, PhD^{1,2}, Takeharu Hayashi, MD, PhD^{*,1,3}, Young E. Jeon, BS^{*,1,3}, Zhenxing Fu, PhD², Yusu Gu, MD², Nancy D. Dalton, RDCS², Mark H. Ellisman, PhD^{1,3}, Xiao Xiao, PhD⁴, Frank L. Powell, PhD², and John Ross Jr., MD²

¹The Center for Research in Biological Systems, University of California San Diego, 9500 Gilman Dr., La Jolla, CA 92093

²Department of Medicine, University of California San Diego, 9500 Gilman Dr., La Jolla, CA 92093

³National Center for Microscopy and Imaging Research, University of California San Diego, 9500 Gilman Dr., La Jolla, CA 92093

⁴Division of Molecular Pharmaceutics, University of North Carolina Eshelman School of Pharmacy, Chapel Hill, NC 27599

Abstract

Background—The BIO14.6 hamster provides a useful model of hereditary cardiomyopathies and muscular dystrophy. Previous delta-sarcoglycan (δ SG) gene therapy (GT) studies were limited to neonatal and young adult animals, and prevented the development of cardiac and skeletal muscle dysfunction. GT of a pseudo-phosphorylated mutant of phospholamban (S16EPLN) moderately alleviated the progression of cardiomyopathy.

Methods and Results—We treated 4 month-old BIO14.6 hamsters with established cardiac and skeletal muscle diseases intravenously with a serotype-9 adeno-associated viral vector carrying δ SG alone or in combination with S16EPLN. Prior to treatment at age 14 weeks, the left ventricular (LV) fractional shortening by echocardiography was 31.3% vs. 45.8% in normal hamsters. In a randomized trial, GT halted progression of LV dilation and LV dysfunction. Also, respiratory function improved. Addition of S16EPLN had no significant additional effects. δ SG-GT prevented severe degeneration of the transverse tubular system in cardiomyocytes (electron tomography), and restored distribution of dystrophin and caveolin-3. All placebo-treated hamsters, except animals removed for the hemodynamic study, died with heart failure between 34 and 67 weeks of age. In the GT group, signs of cardiac and respiratory failure did not develop, and animals lived for 92 weeks or longer, an age comparable to that reported in normal hamsters.

Correspondence to: Masahiko Hoshijima, University of California San Diego, 9500 Gilman Dr., #0734, La Jolla, CA 92093-0734, Tel: 858-822-3422, Fax: 858-534-6974, mhoshijima@ucsd.edu.

*Contributed equally.

Disclosures

None.

This is a PDF file of an unedited manuscript that has been accepted for publication. As a service to our customers we are providing this early version of the manuscript. The manuscript will undergo copyediting, typesetting, and review of the resulting proof before it is published in its final citable form. Please note that during the production process errors may be discovered which could affect the content, and all legal disclaimers that apply to the journal pertain.

Conclusions—GT was highly effective in BIO14.6 hamsters even when given in late stage disease, a finding that may carry implications for the future treatment of hereditary cardiac and muscle diseases in humans.

Keywords

gene therapy; cardiomyopathy; muscles; heart failure; ventilation

Inherited forms of muscular dystrophy including the Duchenne/Becker Muscular Dystrophies (DMD/BMD) (i.e. dystrophinopathies) and Limb-Girdle Muscular Dystrophies (LGMDs) commonly affect both skeletal and cardiac muscles¹. While progressive weakness of neck, trunk, and limb muscles are disabling in such patients, cardiac complications and respiratory failure are major determinants of prognosis^{2,3}. Among the genes mutated in inherited muscular dystrophies, most encode membrane-cytoskeletal proteins that constitute a macro-molecular complex termed the dystrophin-glycoprotein complex (DGC)¹.

BIO14.6 hamsters have a spontaneous genetic deletion around the first exon of the δ -sarcoglycan (δ SG) gene^{4,5}, mutations of which have been linked to human LGMD type 2F¹. Due to the absence of δ SG, BIO14.6 hamsters are unable to form the sarcoglycan (SG) protein complex, a subcomponent of the DGC, on the sarcolemma. Although BIO14.6 hamsters appear normal when born, they die early, with life-span of approximately 12 months, primarily due to the development of severe congestive heart failure⁶.

Phenotypic consistency has made the BIO14.6 hamster a preferred animal model of muscular dystrophy and hereditary cardiomyopathy used for testing new therapies, including gene replacement using viral vectors⁷⁻¹². However, previous experimental trials of gene therapy (GT) in BIO14.6 hamsters⁷⁻¹² and one trial in mice¹³ have focused on the short or long-term effectiveness of disease prevention by treating SG deficiency early in life (neonatal and young adult animals, up to 9 weeks of age), and the effects of GT in late stage disease, when cardiac and respiratory dysfunction are well established, have not been examined.

In the present study, we delivered the δ SG gene using an adeno-associated virus serotype 9 (AAV9) vector by intravenous bolus injection, allowing us to test the efficacy of GT in both the cardiac and skeletal muscles in 4 month old BIO14.6 hamsters with well established cardiac and respiratory failure. In addition, since a substantial number of cardiomyocytes are lost by 4 months of age^{14,15} and surviving cells are under stress, we added an additional group of BIO14.6 hamsters in which GT with a pseudo-phosphorylated mutant (S16E) of phospholamban (PLN) was combined with δ SG GT. Based on our previous studies in BIO14.6 hamsters¹⁶ and post-infarction rats¹⁷, we expected that the positive inotropic effect of S16EPLN treatment could further enhance any benefits from δ SG GT alone.

Methods

Additional details are available on-line in “Expanded Methods”.

Animals

Male BIO14.6 hamsters and golden Syrian hamsters were obtained from Bio Breeders Inc (Watertown, MA). All animal-related procedures were reviewed and approved by the Institutional Animal Care and Use Committee of the University of California San Diego.

Viral vectors

The same δ SG and S16EPLN expression module that was prepared in our previous studies ¹¹ was utilized.

Gene transfer procedures

BIO14.6 hamsters (80-100 gram body weight) were anesthetized with ketamine (100 mg/Kg) and xylazine (2.5 mg/kg). Through a small incision in the left inguinal region, the femoral vein was exposed and cannulated with flame-stretched polyethylene tubing (PE-50, Becton-Dickinson, Parsippany, NJ) and AAV9 vectors (8×10^{11} viral genome particles per 100 gram of body weight) were delivered.

Assessment of cardiac function

The methods for transthoracic echocardiographic analysis of left ventricular (LV) function and retrograde LV catheterization using a micro-manometer in anesthetized hamsters have been described ¹⁸. Examiners were blinded to the treatments.

Assessment of respiratory function

A barometric method of plethymography with continuous flow ¹⁹ was used to calculate tidal volume and minute ventilation in spontaneously breathing, non-anesthetized hamsters. Hypercapnia-induced ventilation estimated the additional capacity of animals to respond to a ventilatory stimulus.

Electron microscopy

The sample preparation procedures have been described ²⁰. Electron tomography was obtained in thick sections (500 nm) using an intermediate high-voltage EM system (400 kV). The tomographic reconstruction was carried out as described ²⁰.

Immuno-fluorescent staining

Snap-frozen heart tissues were cryo-sectioned and unfixed specimens were stained using an indirect immuno-fluorescence strategy as described ¹⁸.

Statistics

Comparison between groups used a mixed-effects linear model or a repeated-measures two-factor ANOVA with post hoc tests. Values are mean \pm SEM, unless stated differently.

Results

The study design is shown in Figure 1A. We treated 16-week old male BIO14.6 hamsters with intravenous injection of an AAV9 vector carrying a human copy of the δ SG gene (δ SG/AAV9), δ SG/AAV9 in combination with S16EPLN carried by an AAV9 vector (S16EPLN/AAV9), and placebo (saline injection). S16EPLN treatment was shown in our previous study to be moderately effective in reducing the degree of heart failure in BIO14.6 hamsters over 7 months ¹⁶. We chose saline-treatment as control based on a finding that echocardiography detected no functional difference between saline-treated animals and animals treated with an AAV9 vector carrying lacZ β -D-galactosidase (n=5 each group) over 6 months (data not shown).

AAV9 vectors are known to effectively transduce genes in cardiac muscle ²¹⁻²⁴. Prior to gene transfer, echocardiographic assessment at 14 weeks of age confirmed that left ventricular (LV) function in these BIO14.6 hamsters was substantially depressed compared to age-matched normal golden Syrian hamsters: the % fractional shortening (%FS) was

31.3±4.89% in the BIO14.6 (n=30) vs. 45.8±2.85% in the normal controls (n=6), (P<0.001) (Figure 2A, Pre). Enlargement of the LV chamber was not yet statistically significant at this age (Figure 2B, Pre). However, the LV end-diastolic wall stress estimated by the LV end-diastolic dimension/posterior wall thickness ratio (LVEDd/PWTh) in BIO14.6 hamsters¹⁶ was twice that in normal hamster (7.19±0.15, n=30, vs. 3.78±0.20, normal hamsters, n=6, P<0.001) (Figure 2D). No early mortality or procedure-related health problems were observed after the gene transfer procedure.

The efficiency of δ SG replacement was nearly 100% both in ventricular cardiomyocytes (Figure 1C and D) and in fast-twitch skeletal muscles including quadriceps (Figure 1F), anterior tibial, and extensor digitorum longus muscle (data not shown). The efficiency was slightly lower in slow-twitch muscles, such as soleus (Figure 1G). No δ SG expression was detectable in non-muscle organs/tissues including liver, lung, kidney, and brain (Figure 1H-K), and the LV coronary vascular system was devoid of staining.

δ SG gene transfer halted the development of cardiac failure

After initial echocardiographic studies, the hamsters were randomly separated into subgroups (10 δ SG/AAV9-treated animals, 10 δ SG/AAV9 and S16EPLN/AAV9-treated, and 10 saline-treated placebo animals) (Figure 1A).

Placebo-treated group—By 25 weeks after placebo treatment, the general health of the BIO14.6 hamster in the placebo was deteriorating, by developing physical weakness including markedly reduced spontaneous activity and poor appetite, and clinical signs of congestive heart failure including dyspnea and anasarca.

One animal died at 18 weeks after the placebo-treatment, and the %FS of the other placebo animals had declined by 25 weeks by an average of 56%, to 13.8±2.13% (n=9) (Figure 2A). The placebo group developed severe LV chamber dilation (Figure 2B). The LV wall thickness remained markedly thinned (Figure 2C), and therefore the estimated diastolic wall stress continuously increased in this group (Figure 2D). Late echocardiographic studies (49 and 65 weeks after treatment) were not obtained for the placebo group. After 5 randomly selected animals were, as scheduled, removed and used for a hemodynamic study at 28 weeks together with other GT-treated animals, all remaining placebo animals died or were severely morbid by the time of the late echocardiography.

GT Groups—Both BIO14.6 hamsters treated with δ SG/AAV9 alone and those treated with δ SG/AAV9 and S16PLN/AAV9 showed vigorous spontaneous activity, maintained good appetite, and displayed no obvious appearance of systemic edema or respiratory distress.

Echocardiography at 25 weeks after GT showed that treatment preserved LV function remarkably well in both treatment groups, demonstrating complete prevention of a decline in the %FS (Figure 2A), suppression of progressive LV dilation (Figure 2B), and a significant increase in diastolic LV wall thickness (Figure 2C) which reduced the estimated LV diastolic wall stress relative to the placebo group (Figure 2D). The rate of decline in %FS and the rate of LV dilation were significantly smaller in the treatment groups than in the placebo (P<0.0001), but there was not a statistically significant difference between the δ SG/AAV9-treatment alone and the combined treatment of δ SG/AAV9 and S16PLN/AAV9 (%FS, P=0.21; LVEDd, P=0.10). LV wall thickness was significantly greater at 25 weeks in the treatment groups than in placebo (δ SG/AAV9 alone, P=0.002; δ SG/AAV9 and S16PLN/AAV9, P=0.0125). Estimated diastolic wall stress did not change significantly after GT (at 25 weeks vs. pre: δ SG/AAV9 alone, P=0.73; δ SG/AAV9 and S16PLN/AAV9, P=0.17).

Late-stage echocardiography (49 and 65 weeks after GT) showed that a favorable effect of the δ SG replacement therapy on cardiac function was maintained. Only mild fall in the %FS (Figure 2A) and gradual LV chamber enlargement (Figure 2B) were recognized.

In animal groups treated with δ SG/AAV9 alone and with δ SG/AAV9 and S16EPLN/AAV9, a beneficial increase in LV wall thickness observed at 25 weeks (see above), might have served to prevent LVEDd/PWTh from increasing significantly at 49 and 65 weeks (Figure 2D).

Hemodynamic Studies—To confirm that prevention of the progressive heart failure phenotypes by GT was due, at least in part, to a direct beneficial effect on LV function and myocardial contractility, BIO14.6 hamsters from each treatment group (n=5 per group) were subjected to invasive cardiac hemodynamic examination (catheter tip micromanometry) at 28 weeks after GT (at age 44 weeks) (Figure 3). At rest and with a treatment of increasing doses of dobutamine, the maximum first derivative of LV pressure (max LV dP/dt), an index of LV myocardial contractility, was significantly higher in both of the treated groups compared to the placebo group (Figure 3A). GT also caused marked enhancement of LV relaxation, reflected in an increase in the peak negative first derivative of LV pressure (min LV dP/dt) (Figure 3C) and a shorter time constant of LV pressure decay (τ) (Figure 3D), a relatively load independent measure of relaxation.

δ SG gene transfer halted deterioration of respiratory function

Most of the placebo-treated BIO14.6 hamsters showed clinical signs of severe respiratory distress before they died. Although lung congestion secondary to heart failure can be the cause of dyspnea, respiratory muscles are among the most severely affected skeletal muscles in BIO14.6 hamsters^{14, 15}. Therefore, we combined the 84-86 weeks old δ SG/AAV9-treated animals with (n=4) and without (n=3) S16EPLN treatment and applied whole body plethysmography in wake animals breathing spontaneously. Because untreated BIO14.6 hamsters do not survive to this age, we studied 42-46 weeks old BIO14.6 hamsters as controls without GT. Golden Syrian hamsters (42-46 weeks old) served as normal controls.

Untreated group—Basal respiratory function (tidal volume and minute ventilation) was mildly depressed in the non-treated group compared to normal hamsters (Figure 4 A and B). However, the hypercapnic ventilatory response to 8% CO₂ was severely impaired. The tidal volume increased by only 45%, compared to highly significant increases (81%) in normal hamsters (Figure 4A). Hypercapnia also inefficiently stimulated minute ventilation of non-treated BIO14.6 hamsters (Figure 4B).

GT group—The basal tidal volume of GT-treated BIO14.6 hamsters was not significantly different from that in normal hamsters (Figure 4A). In 8% CO₂, tidal volume increased by 66% and minute ventilation increased by 117%, to a functional level that was not significantly different from that measured in younger normal hamsters (Figure 4 A and B). There was no significant difference between the three animal groups (normal hamsters, BIO14.6 hamsters, and GT-treated BIO14.6 hamsters) with respect to respiratory frequency, both at rest and after receiving hypercapnic stimulation.

Efficiency of δ SG replacement in respiratory muscles—GT restored δ SG in respiratory muscles (diaphragm and the intercostal muscle: ICM), and efficiency was nearly 100% in ICM (Figure 4D and H), although δ SG expression was lower and inhomogeneous in the diaphragm (Figure 4F and J). In addition, α SG and β SG immuno-staining was observed on the sarcolemma in treated BIO14.6 hamsters (data not shown), confirming that the SG complex was restored on the sarcolemma in respiratory muscles.

δSG gene transfer preserved ultrastructure and subcellular components in cardiac muscle

Degeneration of the transverse tubular system (T system) was ameliorated—

δSG is known to localize both on the peripheral sarcolemma and along the T system^{25, 26} (Figure 1C and D). Therefore, using an advanced 3-dimensional (3-D) electron microscopic technology (electron tomography), we characterized T system abnormality, which was previously reported²⁷.

As shown in Figure 5D and F (see also Video 1), high-resolution electron tomography (voxel size: 1.42 nm × 1.42 nm × 1.42 nm) revealed a strikingly deformed cardiac T system in placebo-treated BIO14.6 hamsters. Interestingly, multiple cystic invaginations with diameters of 75-100 nm were observed on T system membranes (Figure 5F). Such T system abnormalities were absent in BIO14.6 hamsters treated with δSG replacement (Figure 5 C, E, and G).

DGC was reconstituted—Despite preceding focal lytic changes in the myocardium, δSG GT effectively recruited and stabilized αSG (Figure 6 C and F), as well as βSG and γSG (data not shown), on the sarcolemma of surviving cardiomyocytes; the SGs were restored on both the peripheral sarcolemma and the internal sarcolemma of the T system. δSG replacement also favorably affected the entire DGC, including the correction of the abnormal distribution of dystrophin at intercalated discs (Figure 6 I and H), which was reported previously¹⁸. β-dystroglycan (β-DG) is considered to serve as an intermediate molecule connecting the SG complex and dystrophin¹; however, the subcellular distribution of β-DG (Figure 6 J-L) did not coincide with dystrophin redistribution (Figure 6 G-I).

δSG GT prevented changes in caveolin-3 (Cav3) distribution—Because the multiple micro cystic invaginations of the T system membranes found on electron tomography resemble caveolae (see Discussion), we analyzed the distribution of Cav3, a key molecule in the formation of caveolae in cardiac muscle²⁸ using immuno-staining. Unexpectedly, T system-associated Cav3 staining was greatly reduced in untreated BIO14.6 hamsters, while the punctate staining pattern of Cav3 along the peripheral sarcolemma remained (Figure 7 B, E, and H). This abnormal Cav3 distribution was not seen in the δSG/ AAV9-treated BIO14.6 hamsters (Figure 7 C, F, and I).

GT prolonged the lifespan of BIO14.6 hamsters

As noted above, due to the development of severe symptoms of cardiac and respiratory failures, none of placebo-treated BIO14.6 hamsters (n=5) survived to undergo late echocardiography. These animals died of the heart failure between 34 and 67 weeks of age. In contrast, there was no animal loss in the GT-treated groups (n=10) until one animal was found dead at 92 weeks of age, followed by two animals at 93 weeks. These animals showed gradual reduction of activity but did not present obvious signs of heart failure or respiratory distress. Kaplan-Meier analysis with the log-rank test revealed significant improvement in animal survival in the treatment groups (each group, P=0.004). The addition of S16EPLN/ AAV9 treatment provided no additional benefit (P=0.48). It should be noted that the late deaths at 92 and 93 weeks are within the reported lifespan of the normal Syrian hamster, 82±25 weeks in one study²⁹ and 106±26 weeks (mean±SD) in another study³⁰. The remaining 7 animals in the GT group were euthanized at 96 weeks in order to perform tissue studies.

Discussion

While previous gene therapy trials treated young BIO14.6 hamsters and δSG-null mice before the onset or at an early stage of the disease⁷⁻¹³, we chose 16 weeks of age in the

current study as the time for GT in BIO14.6 hamsters when LV dysfunction is moderately severe¹⁸. In the BIO14.6 hamster, the lytic changes in the myocardium and respiratory muscles become evident by 20-40 days of age¹⁵ and subside by 150-160 days to be replaced by fibrosis and calcification^{14, 15}. The progression of cardiac and skeletal muscle weakness lags somewhat behind histological changes^{14, 15}. For example, the LV was not significantly dilated and the %FS was only mildly reduced (37-40%) just prior to treatment in our previous δ SG GT trial in 7 to 9 week old BIO14.6 hamsters⁸. In addition, myopathic changes do not appear until 3 months of age in δ SG-null mice³¹, which were treated in a previous GT study¹³. Accordingly, this study appears to be the first to show that GT at a relatively advanced stage of disease in this form of hereditary cardiac and skeletal myopathy can halt the rapid progression of clinical signs and echocardiographic findings of LV dysfunction, ameliorate many of the structural abnormalities in cardiac muscle, and favorably affect survival.

We consider that the failure of the S16EPLN treatment to provide an additional effect in the current study is primarily due to the overwhelming efficacy of δ SG GT. In addition, the efficacy of S16EPLN therapy is sensitive to the stoichiometry of sarcoplasmic reticulum calcium-ATPase and native PLN molecules¹⁶, which might not be optimal in the current study, where recipient BIO14.6 hamsters were much later into treatment than in our earlier study¹⁶.

We believe that this study provides the initial demonstration of a successful *in vivo* treatment of respiratory dysfunction by GT in a muscular dystrophy model. Since cardiac function and lung function are highly interrelated^{32, 33}, we speculate that the improvement of respiratory function found in the current study is probably due to both a direct effect of GT on respiratory muscles and a secondary effect from improved cardiac function.

The study also applied electron tomography^{20, 34} and revealed an enormous T-system dilation and multiple small cystic invaginations associated with the T-system in placebo-treated BIO14.6 hamsters (Figure 5 D and F). From their size and shape, we initially speculated that these cystic membrane structures represented caveolae^{35, 36}. Caveolae are frequently observed on the peripheral sarcolemma of cardiac myocytes³⁵ and at the tips of elongating cardiac T-tubules in young mammals³⁷. In the past, caveolae were thought to be the precursor of T-tubules³⁸. However, this is unlikely in this case, since Cav3, which is prerequisite for caveola formation in striated muscles²⁸, was found to be dissociated from the T system in BIO14.6 hamsters (Figure 7 E and H). The cause of Cav3 dislocation is not clear, as Cav3 may not be an integral component of the DGC³⁹. Nonetheless, it remains possible that the translocation of Cav3 might be a factor leading to disorganization of the cardiac T system in BIO14.6 hamsters, as suggested in studies in humans with LGMD⁴⁰.

There is an increasing awareness of the clinical importance of cardiac involvement in muscular dystrophy^{2, 3}. Currently, cardiac and skeletal muscles are often significantly damaged when patients are first diagnosed, despite increasing use of newborn screening⁴¹. The δ SG-deficient BIO14.6 hamster used in the current study develops myolysis and progressive weakness in both cardiac and skeletal muscles resembling the clinical manifestation of DMD/BMD. Also, plasma membrane fragility has been suggested as the central disease mechanism of dystroglycanopathies and genetic SG defects, as recently reviewed¹. Importantly, recent improvements in health care practices have extended the lifespan of DMD/BMD patients and, as a result, nearly 90% of DMD/BMD patients now die from cardiac or muscular respiratory failure². Accelerated cardiac damage found in dystrophin-deficient mice that were selectively treated for skeletal muscle myopathy further supports the need for cardiac therapy in muscular dystrophy⁴². In addition, approximately 25% of all so-called idiopathic cardiomyopathies in humans are genetic, and these

individuals might not be identified at an early disease stage by family studies and/or genetic screening⁴³. Therefore, we consider that the therapeutic efficacy of relatively late gene replacement demonstrated in the present study carries significant clinical implications for the future of GT in humans, even when cardiac and respiratory dysfunction are well established.

Supplementary Material

Refer to Web version on PubMed Central for supplementary material.

Acknowledgments

We are grateful to Drs. Colleen Kelly and Karen Messer (Moores UCSD Cancer Center Biostatistics and Bioinformatics) for thorough statistics assistance, and Dr. Moh Malek for statistical advice. We are indebted to Tapaswani Das and Andrea Thor for technical assistance.

Sources of Funding

A Muscular Dystrophy Foundation grant to Dr. Ross (MDA3758) supported this work. NIH grants supported Dr. Xiao (R01AR045967) and Dr. Powell (R01HL081823). An NIH/National Center for Research Resources grant to Dr. Ellisman supported microscopy studies (P41RR004050). Dr. Hoshijima is partly supported by American Heart Association Established Investigator Award (0840013N).

References

1. McNally EM, Pytel P. Muscle diseases: the muscular dystrophies. *Annu Rev Pathol.* 2007; 2:87–109. [PubMed: 18039094]
2. Finsterer J. Cardiopulmonary support in duchenne muscular dystrophy. *Lung.* 2006; 184:205–215. [PubMed: 17006747]
3. Wagner KR, Lechtzin N, Judge DP. Current treatment of adult Duchenne muscular dystrophy. *Biochim Biophys Acta.* 2007; 1772:229–237. [PubMed: 16887341]
4. Nigro V, Okazaki Y, Belsito A, Piluso G, Matsuda Y, Politano L, Nigro G, Ventura C, Abbondanza C, Molinari AM, Acampora D, Nishimura M, Hayashizaki Y, Puca GA. Identification of the Syrian hamster cardiomyopathy gene. *Hum Mol Genet.* 1997; 6:601–607. [PubMed: 9097966]
5. Sakamoto A, Ono K, Abe M, Jasmin G, Eki T, Murakami Y, Masaki T, Toyo-oka T, Hanaoka F. Both hypertrophic and dilated cardiomyopathies are caused by mutation of the same gene, delta-sarcoglycan, in hamster: an animal model of disrupted dystrophin-associated glycoprotein complex. *Proc Natl Acad Sci U S A.* 1997; 94:13873–13878. [PubMed: 9391120]
6. Homburger F. Myopathy of hamster dystrophy: history and morphologic aspects. *Ann N Y Acad Sci.* 1979; 317:1–17. [PubMed: 382952]
7. Holt KH, Lim LE, Straub V, Venzke DP, Duclos F, Anderson RD, Davidson BL, Campbell KP. Functional rescue of the sarcoglycan complex in the BIO 14.6 hamster using delta-sarcoglycan gene transfer. *Mol Cell.* 1998; 1:841–848. [PubMed: 9660967]
8. Ikeda Y, Gu Y, Iwanaga Y, Hoshijima M, Oh SS, Giordano FJ, Chen J, Nigro V, Peterson KL, Chien KR, Ross J Jr. Restoration of deficient membrane proteins in the cardiomyopathic hamster by in vivo cardiac gene transfer. *Circulation.* 2002; 105:502–508. [PubMed: 11815435]
9. Kawada T, Nakazawa M, Nakauchi S, Yamazaki K, Shimamoto R, Urabe M, Nakata J, Hemmi C, Masui F, Nakajima T, Suzuki J, Monahan J, Sato H, Masaki T, Ozawa K, Toyo-Oka T. Rescue of hereditary form of dilated cardiomyopathy by rAAV-mediated somatic gene therapy: amelioration of morphological findings, sarcolemmal permeability, cardiac performances, and the prognosis of TO-2 hamsters. *Proc Natl Acad Sci U S A.* 2002; 99:901–906. [PubMed: 11805334]
10. Li J, Wang D, Qian S, Chen Z, Zhu T, Xiao X. Efficient and long-term intracardiac gene transfer in delta-sarcoglycan-deficiency hamster by adeno-associated virus-2 vectors. *Gene Ther.* 2003; 10:1807–1813. [PubMed: 12960970]

11. Zhu T, Zhou L, Mori S, Wang Z, McTiernan CF, Qiao C, Chen C, Wang DW, Li J, Xiao X. Sustained whole-body functional rescue in congestive heart failure and muscular dystrophy hamsters by systemic gene transfer. *Circulation*. 2005; 112:2650–2659. [PubMed: 16230483]
12. Vitiello C, Faraso S, Sorrentino NC, Di Salvo G, Nusco E, Nigro G, Cutillo L, Calabro R, Auricchio A, Nigro V. Disease rescue and increased lifespan in a model of cardiomyopathy and muscular dystrophy by combined AAV treatments. *PLoS One*. 2009; 4:e5051. [PubMed: 19333401]
13. Goehringer C, Rutschow D, Bauer R, Schinkel S, Weichenhan D, Bekeredjian R, Straub V, Kleinschmidt JA, Katus HA, Muller OJ. Prevention of cardiomyopathy in delta-sarcoglycan knockout mice after systemic transfer of targeted adeno-associated viral vectors. *Cardiovasc Res*. 2009; 82:404–410. [PubMed: 19218289]
14. Strobeck JE, Factor SM, Bhan A, Sole M, Liew CC, Fein F, Sonnenblick EH. Hereditary and acquired cardiomyopathies in experimental animals: mechanical, biochemical, and structural features. *Ann N Y Acad Sci*. 1979; 317:59–88. [PubMed: 157709]
15. Jasmin G, Proschek L. Hereditary polymyopathy and cardiomyopathy in the Syrian hamster. I. Progression of heart and skeletal muscle lesions in the UM-X7.1 line. *Muscle Nerve*. 1982; 5:20–25. [PubMed: 7057801]
16. Hoshijima M, Ikeda Y, Iwanaga Y, Minamisawa S, Date MO, Gu Y, Iwatate M, Li M, Wang L, Wilson JM, Wang Y, Ross J Jr. Chronic suppression of heart-failure progression by a pseudophosphorylated mutant of phospholamban via in vivo cardiac rAAV gene delivery. *Nat Med*. 2002; 8:864–871. [PubMed: 12134142]
17. Iwanaga Y, Hoshijima M, Gu Y, Iwatate M, Dieterle T, Ikeda Y, Date MO, Chrast J, Matsuzaki M, Peterson KL, Chien KR, Ross J Jr. Chronic phospholamban inhibition prevents progressive cardiac dysfunction and pathological remodeling after infarction in rats. *J Clin Invest*. 2004; 113:727–736. [PubMed: 14991071]
18. Ikeda Y, Martone M, Gu Y, Hoshijima M, Thor A, Oh SS, Peterson KL, Ross J Jr. Altered membrane proteins and permeability correlate with cardiac dysfunction in cardiomyopathic hamsters. *Am J Physiol Heart Circ Physiol*. 2000; 278:H1362–1370. [PubMed: 10749734]
19. Aaron EA, Powell FL. Effect of chronic hypoxia on hypoxic ventilatory response in awake rats. *J Appl Physiol*. 1993; 74:1635–1640. [PubMed: 8514677]
20. Hayashi T, Martone ME, Yu Z, Thor A, Doi M, Holst MJ, Bajaj CL, Ellisman MH, Hoshijima M. Three-dimensional electron microscopy reveals new details of membrane systems for calcium signaling in the heart. *J Cell Sci*. 2009; 122:1005–13. [PubMed: 19295127]
21. Inagaki K, Fuess S, Storm TA, Gibson GA, McTiernan CF, Kay MA, Nakai H. Robust systemic transduction with AAV9 vectors in mice: efficient global cardiac gene transfer superior to that of AAV8. *Mol Ther*. 2006; 14:45–53. [PubMed: 16713360]
22. Pacak CA, Mah CS, Thattaliyath BD, Conlon TJ, Lewis MA, Cloutier DE, Zolotukhin I, Tarantal AF, Byrne BJ. Recombinant adeno-associated virus serotype 9 leads to preferential cardiac transduction in vivo. *Circ Res*. 2006; 99:e3–9. [PubMed: 16873720]
23. Bostick B, Ghosh A, Yue Y, Long C, Duan D. Systemic AAV-9 transduction in mice is influenced by animal age but not by the route of administration. *Gene Ther*. 2007; 14:1605–1609. [PubMed: 17898796]
24. Yang L, Jiang J, Drouin LM, Agbandje-McKenna M, Chen C, Qiao C, Pu D, Hu X, Wang DZ, Li J, Xiao X. A myocardium tropic adeno-associated virus (AAV) evolved by DNA shuffling and in vivo selection. *Proc Natl Acad Sci U S A*. 2009; 106:3946–3951. [PubMed: 19234115]
25. Heydemann A, McNally EM. Consequences of disrupting the dystrophin-sarcoglycan complex in cardiac and skeletal myopathy. *Trends Cardiovasc Med*. 2007; 17:55–59. [PubMed: 17292047]
26. Brette F, Orchard C. Resurgence of cardiac t-tubule research. *Physiology (Bethesda)*. 2007; 22:167–173. [PubMed: 17557937]
27. Sen LY, O'Neill M, Marsh JD, Smith TW. Myocyte structure, function, and calcium kinetics in the cardiomyopathic hamster heart. *Am J Physiol*. 1990; 259:H1533–1543. [PubMed: 2240250]
28. Williams TM, Lisanti MP. The Caveolin genes: from cell biology to medicine. *Ann Med*. 2004; 36:584–595. [PubMed: 15768830]

29. Tanaka A, Hisanaga A, Ishinishi N. The frequency of spontaneously-occurring neoplasms in the male Syrian golden hamster. *Vet Hum Toxicol.* 1991; 33:318–321. [PubMed: 1897125]
30. Kamino K, Tillmann T, Boschmann E, Mohr U. Age-related incidence of spontaneous non-neoplastic lesions in a colony of Han:AURA hamsters. *Exp Toxicol Pathol.* 2001; 53:157–164. [PubMed: 11484834]
31. Coral-Vazquez R, Cohn RD, Moore SA, Hill JA, Weiss RM, Davisson RL, Straub V, Barresi R, Bansal D, Hrstka RF, Williamson R, Campbell KP. Disruption of the sarcoglycan-sarcospan complex in vascular smooth muscle: a novel mechanism for cardiomyopathy and muscular dystrophy. *Cell.* 1999; 98:465–474. [PubMed: 10481911]
32. Belenkie I, Smith ER, Tyberg JV. Ventricular interaction: from bench to bedside. *Ann Med.* 2001; 33:236–241. [PubMed: 11405544]
33. Agostoni P, Cattadori G, Bussotti M, Apostolo A. Cardiopulmonary interaction in heart failure. *Pulm Pharmacol Ther.* 2007; 20:130–134. [PubMed: 16702004]
34. Yu Z, Holst MJ, Hayashi T, Bajaj CL, Ellisman MH, McCammon JA, Hoshijima M. Three-dimensional geometric modeling of membrane-bound organelles in ventricular myocytes: Bridging the gap between microscopic imaging and mathematical simulation. *J Struct Biol.* 2008; 164:304–313. [PubMed: 18835449]
35. Page, E.; Iida, H.; Doyle, DD. Cell physiology and cell biology of myocardial cell caveolae. In: Page, E.; Fozzard, HA.; Solaro, RJ., editors. Section 2, The Cardiovascular System: Volume I, The Heart. American Physiological Society; Bethesda, Maryland: 2002. p. 145-168.
36. Stan RV. Structure of caveolae. *Biochim Biophys Acta.* 2005; 1746:334–348. [PubMed: 16214243]
37. Forbes MS, Sperelakis N. The presence of transverse and axial tubules in the ventricular myocardium of embryonic and neonatal guinea pigs. *Cell Tissue Res.* 1976; 166:83–90. [PubMed: 942885]
38. Forbes, MS.; Sperelakis, N. Ultrastructure of mammalian cardiac muscle. Physiology and pathophysiology of the heart. In: Sperelakis, N., editor. Kluwer Academic Publishers; Dordrecht, the Netherlands: 1984. p. 3-42.
39. Crosbie RH, Yamada H, Venzke DP, Lisanti MP, Campbell KP. Caveolin-3 is not an integral component of the dystrophin glycoprotein complex. *FEBS Lett.* 1998; 427:279–282. [PubMed: 9607328]
40. Minetti C, Bado M, Broda P, Sotgia F, Bruno C, Galbiati F, Volonte D, Lucania G, Pavan A, Bonilla E, Lisanti MP, Cordone G. Impairment of caveolae formation and T-system disorganization in human muscular dystrophy with caveolin-3 deficiency. *Am J Pathol.* 2002; 160:265–270. [PubMed: 11786420]
41. Kemper AR, Wake MA. Duchenne muscular dystrophy: issues in expanding newborn screening. *Curr Opin Pediatr.* 2007; 19:700–704. [PubMed: 18025940]
42. Townsend D, Yasuda S, Li S, Chamberlain JS, Metzger JM. Emergent dilated cardiomyopathy caused by targeted repair of dystrophic skeletal muscle. *Mol Ther.* 2008; 16:832–835. [PubMed: 18414480]
43. McMinn TR Jr, Ross J Jr. Hereditary dilated cardiomyopathy. *Clin Cardiol.* 1995; 18:7–15. [PubMed: 7704989]

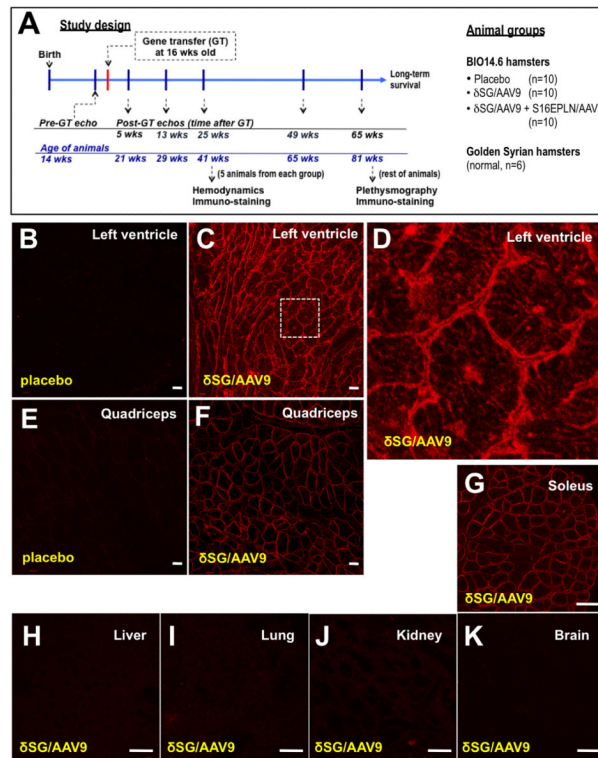


Figure 1. Systemic induction of δ SG in BIO14.6 hamsters using an AAV9 vector

A shows the time course of the study. The human copy of δ SG was systemically transferred intravenously to BIO14.6 hamsters at the age of 16 weeks, with or without a pseudo-phosphorylated mutant PLN (S16EPLN), both carried by an AAV9 vector. GT, gene transfer. B and E show negative δ SG immuno-staining in left ventricular and quadriceps muscles in placebo (saline)-treated BIO14.6 hamsters. C, D, and F-K are representative δ SG immuno-staining in various tissues collected from δ SG/AAV9-treated BIO14.6 hamsters at 28 weeks (wks) after gene transfer. D is a high magnification view of a subarea of C (dashed line square). δ SG induction was confirmed on both the peripheral sarcolemma and the T system (D). Bars, 10 μ m in B-F, 100 μ m in G-K.

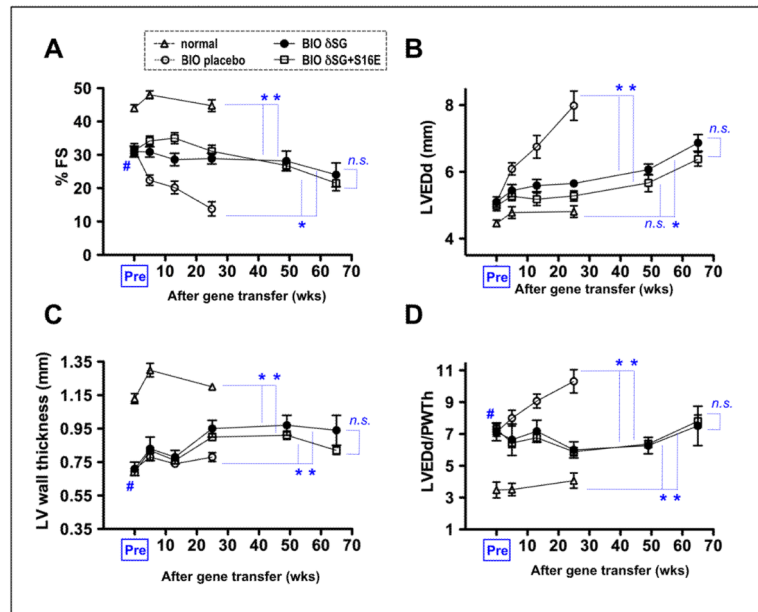


Figure 2. δ SG replacement with S16EPLN therapy prevented the progression of cardiac dysfunction and chamber dilation in BIO14.6 hamsters

Normal, placebo-treated, and BIO14.6 hamsters treated with the δ SG/AAV9 alone or in combination with S16EPLN/AAV9 (denoted as BIO δ SG and BIO δ SG+S16E, respectively) were followed by serial echocardiograms. A shows preservation of %FS with treatment, as an index of LV systolic function. B indicates prevention of LV dilation with treatment. C demonstrates changes in diastolic LV wall thickness. In D, estimated diastolic wall stress (LVEDd/PWTh) is significantly reduced by the treatment (relative to the placebo). See the text for details. The blue dashed lines are pair-wise comparisons between animal groups tested by a mixed-effects linear model (* $P < 0.05$ or “n.s.”). Depressed cardiac function of BIO14.6 hamsters prior to the treatment was shown (# $P < 0.05$, vs. normal at pre-GT). Error bars are means \pm SEM. Pre, pre-GT; n.s., no significance.

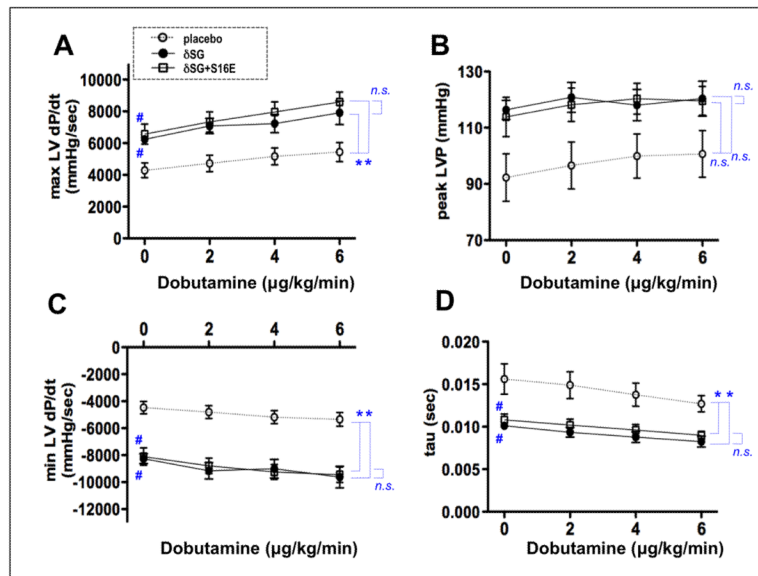


Figure 3. Chronically improved cardiac contractility and relaxation by δSG replacement therapy in BIO14.6 hamsters

BIO14.6 hamsters treated with $\delta\text{SG}/\text{AAV9}$ alone or in combination with S16EPLN/AAV9 (BIO δSG and BIO $\delta\text{SG}+\text{S16E}$, respectively) for 28 weeks were subjected to hemodynamic analyses. At rest (dobutamine, 0 $\mu\text{g/Kg/min}$) measures of LV contractility (max LV dP/dt) shown in A and relaxation (min LV dP/dt and tau) shown in C were significantly higher in treated animals than in placebo-treated controls. Since min LV dP/dt is sensitive to changes in peak LVP, tau (a relatively load-independent index of relaxation) was also evaluated (D) and improved at rest in the GT groups. Dobutamine enhanced LV systolic and diastolic functions dose-dependently in both placebo and GT groups. The blue dashed lines are pairwise comparisons between animal groups (* $P < 0.05$ or “n.s.”). # $P < 0.05$, vs. placebo at rest. Error bars are means \pm SEM. n.s., no significance.

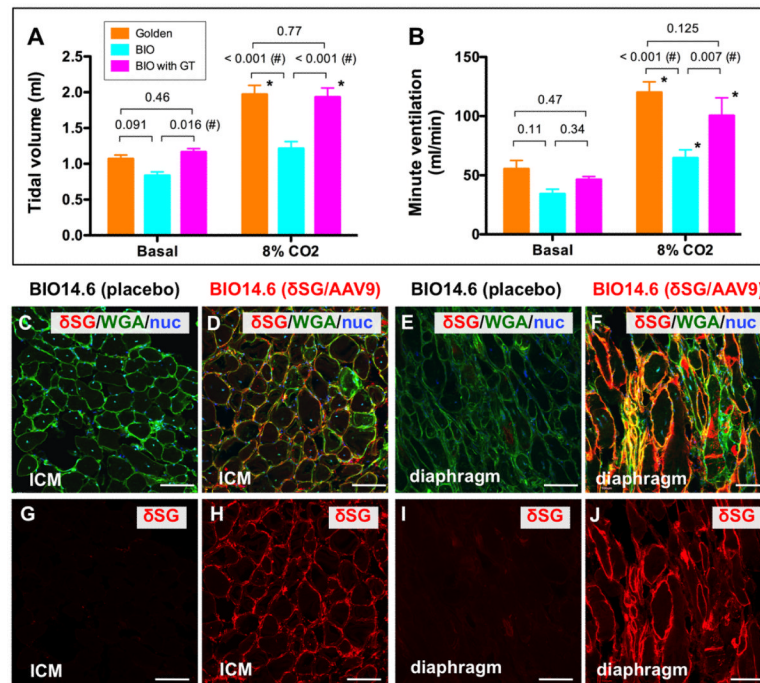


Figure 4. δ SG replacement improved respiratory function and restored the SG complex on the respiratory muscle sarcolemma

A and B show ventilatory function in BIO14.6 hamsters (84-86 weeks old, n=7) treated with δ SG/AAV9 at 16 weeks of age, with and without additional S16EPLN treatment, compared to that of untreated younger BIO14.6 hamsters and normal golden hamsters (42-46 weeks old, n=6 in each group). In both tidal volume (A) and minute ventilation (B) measurements, beneficial therapeutic effects are shown at rest (Basal) and after exposure to hypercapnia (8% CO₂). The mean values of measurements in treated hamsters are statistically indistinguishable from those measured in younger normal hamsters. Unadjusted p-values of pair-wise comparisons are shown in A and B. # p-value is smaller than the critical level of significance. * p-value is smaller than the critical level of significance, vs. basal. The Error bars are means \pm SEM. Representative immuno-staining of restored δ SG is shown in the diaphragm (F and J) and intercostal muscles (ICM, D and H). C, G, E and I show absence of SG staining in placebo-treated BIO14.6 hamsters. G-J show δ SG staining alone. In C-F, sarcolemmal staining with WGA (green) and nuclear staining with DAPI (nuc, blue) are co-visualized. Bars, 100 μ m.

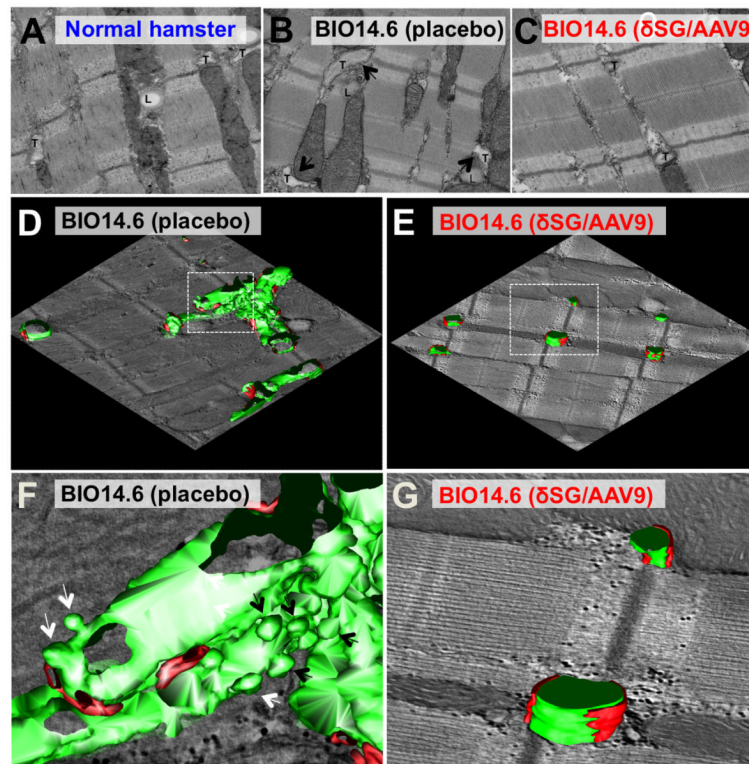


Figure 5. Degeneration of the cardiac T system in BIO14.6 hamsters demonstrated by electron tomography

A-C, 70-nm thin-section electron micrographs. *T*, T-tubule. *L*, lipid droplet. In B, *arrows* indicate dilated T-tubules in BIO14.6 cardiomyocytes treated with placebo for 28 weeks, compared to normal T-tubules found in golden Syrian hamsters (A) and in BIO14.6 cardiomyocytes treated with δ SG/AAV9 alone (C). D-G are composite images of 3-D surface-rendered mesh models of T system (green) and dyadic junctions (red) with 2-dimensional slices, generated from reconstructed electron tomograms. F and G are high magnification views of outlined volumes in D and F (white dashed lines), respectively. *Arrows* in F indicate multiple “caveola”-like cystic invaginations of the T system membrane. The size of tomograms is $5.8 \times 5.4 \times 0.36 \mu\text{m}^3$ (placebo) and $5.8 \times 5.5 \times 0.27 \mu\text{m}^3$ (δ SG treated), respectively. See Video 1.

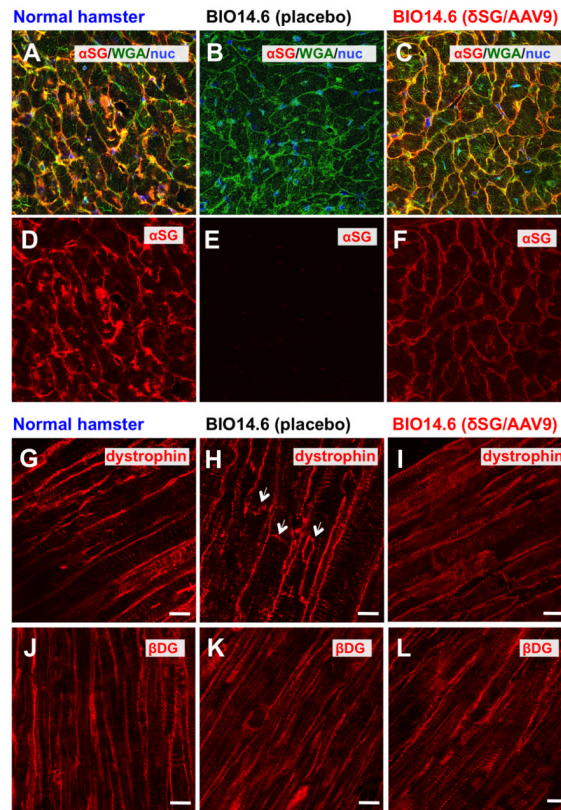


Figure 6. Reconstitution of the DGC by δ SG GT in cardiomyocytes

LV tissues were collected from BIO14.6 hamsters after 28-weeks of treatment with δ SG/AAV9 alone. The effect of δ SG/AAV9 treatment (C, F, I, and L) in BIO14.6 hamsters was referenced to placebo treatment (B, E, H, and K) and normal golden Syrian hamsters (A, D, G, and J). D-F show α SG staining (red) alone. A-C show combination of α SG staining (red) with membrane staining with WGA (green), which stains both the peripheral sarcolemma and T system, and nuclear staining (nuc, blue) with DAPI. G-I shows that dystrophin is expressed on both the peripheral sarcolemma and T system, and aberrantly expressed in intercalated discs only in placebo-treated BIO14.6 cardiomyocytes (H, *arrows*). The dystrophin expression in intercalated discs was not accompanied by change in β -DG distribution (K). Bars, 10 μ m.

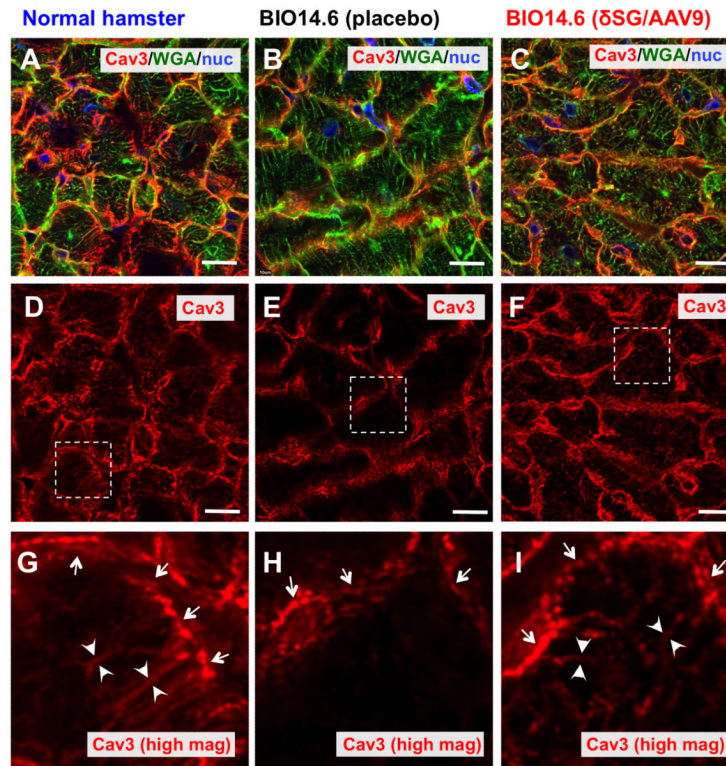


Figure 7. Aberrant distribution of Cav3 in BIO14.6 hamster cardiomyocytes, which was restored by δ SG replacement

A-C show Cav3 immuno-staining (red), together with sarcolemmal staining with WGA (green) and nuclear staining with DAPI (nuc, blue). D-I are Cav3 immuno-staining only (red). G-I represent high magnification of D-F, respectively (dashed line square). The system-associated distribution of Cav3 in normal hamsters (*arrow heads* in G) is largely lost in cardiomyocytes in 28-week placebo-treated BIO4.6 hamsters (E and H). Punctate Cav3 staining on the peripheral sarcolemma (*arrows* in G-I) is, on the other hand, preserved (H). Abnormal Cav3 distribution was restored at 28-weeks after δ SG replacement (F and I). Bars, 10 μ m.